Real-time monitoring of superoxide anion radical generation in response to wounding: electrochemical study

Ankush Prasad [Corresp., 1, 2] , **Aditya Kumar** [1] , **Ryo Matsuoka** [3] , **Akemi Takahashi** [4] , **Ryo Fujii** [4] , **Yamato Sugiura** [4] , **Hiroyuki Kikuchi** [4] , **Shigeo Aoyagi** [3] , **Tatsuo Aikawa** [5] , **Takeshi Kondo** [5] , **Makoto Yuasa** [5] , **Pavel Pospíšil** [1] , **Shigenobu Kasai** [2, 4]

[1] Department of Biophysics, Centre of the Region Haná for Biotechnological and Agricultural Research, Faculty of Science, Palacký University, Olomouc, Czech Republic

[2] Biomedical Engineering Research Center, Tohoku Institute of Technology, Sendai, Japan

[3] Hokuto Denko Corporation, Tokyo, Japan

[4] Graduate Department of Environmental Information Engineering, Tohoku Institute of Technology, Sendai, Japan

[5] Department of Pure and Applied Chemistry, Tokyo University of Science, Noda, Chiba, Japan

Corresponding Author: Ankush Prasad
Email address: prasad.ankush@gmail.com

Background: The growth and development of plants are deleteriously affected by various biotic and abiotic stress factors. Wounding in plants is caused by exposure to environmental stress, mechanical stress, and via herbivory. Typically, oxidative burst in response to wounding is associated with the formation of reactive oxygen species, such as the superoxide anion radical ($O_2^{\bullet-}$), hydrogen peroxide (H_2O_2) and singlet oxygen; however, few experimental studies have provided direct evidence of their detection in plants. Detection of $O_2^{\bullet-}$ formation in plant tissues have been performed using various techniques including electron paramagnetic resonance spin-trap spectroscopy, epinephrine-adrenochrome acceptor methods, staining with dyes such as tetrazolium dye and nitro blue tetrazolium (NBT), however, kinetic measurements have not been performed. In the current study, we provide evidence of $O_2^{\bullet-}$ generation and its kinetics in the leaves of spinach (Spinacia oleracea) subjected to wounding.

Methods: Real-time monitoring of $O_2^{\bullet-}$ generation was performed using catalytic amperometry. Changes in oxidation current for $O_2^{\bullet-}$ was monitored using polymeric iron-porphyrin-based modified carbon electrodes (φ=1 mm) as working electrode with Ag/AgCl as the reference electrode.

Result: The results obtained show a continuous generation of generation of $O_2^{\bullet-}$ for minutes after wounding, followed by a decline. The exogenous addition of superoxide dismutase, which is known to dismutate $O_2^{\bullet-}$ to H_2O_2, significantly suppressed the oxidation current.

Conclusion: Catalytic amperometric measurements were performed using polymeric iron-porphyrin based modified carbon electrode. It is claimed to be a useful tool and a direct method for real-time monitoring and precise detection of $O_2^{\bullet-}$ in biological samples. It is claimed to bear a potential for its wide application in plant research for specific and sensitive detection of $O_2^{\bullet-}$.

1 **Real-time monitoring of superoxide anion radical generation in**

2 **response to wounding: electrochemical study**

3 Ankush Prasad[1,2*], Aditya Kumar[1], Ryo Matsuoka[3], Akemi Takahashi[4], Ryo Fujii[4], Yamato

4 Sugiura[4], Hiroyuki Kikuchi[4], Shigeo Aoyagi[3], Tatsuo Aikawa[5], Takeshi Kondo[5], Makoto Yuasa[5],

5 Pavel Pospíšil[1], Shigenobu Kasai[#2,4]

8 [1]Department of Biophysics, Centre of the Region Haná for Biotechnological and Agricultural

9 Research, Faculty of Science, Palacký University, Olomouc, Czech Republic

10 [2]Biomedical Engineering Research Center, Tohoku Institute of Technology, Sendai, Japan.

11 [3]Hokuto Denko Corporation, Tokyo, Japan

12 [4]Graduate Department of Environmental Information Engineering, Tohoku Institute of

13 Technology, Sendai, Japan.

14 [5]Department of Pure and Applied Chemistry, Tokyo University of Science,

15 Noda, Chiba, Japan

19 *Corresponding author: Ankush Prasad, Department of Biophysics, Centre of the Region Haná

20 for Biotechnological and Agricultural Research, Faculty of Science, Palacký University,

21 Šlechtitelů 27, 783 71 Olomouc, Czech Republic.

22 Tel. +420-58563-4752; fax: +420 585225737; E-mail address: ankush.prasad@upol.cz

23 [#]Co-corresponding author: kasai@tohtech.ac.jp

25 **ABSTRACT**

Background:

27 The growth and development of plants are deleteriously affected by various biotic and abiotic

28 stress factors. Wounding in plants is caused by exposure to environmental stress, mechanical

29 stress, and via herbivory. Typically, oxidative burst in response to wounding is associated with

30 the formation of reactive oxygen species, such as the superoxide anion radical ($O_2^{\bullet-}$), hydrogen

31 peroxide (H_2O_2) and singlet oxygen; however, few experimental studies have provided direct

32 evidence of their detection in plants. Detection of $O_2^{\bullet-}$ formation in plant tissues have been

33 performed using various techniques including electron paramagnetic resonance spin-trap

34 spectroscopy, epinephrine-adrenochrome acceptor methods, staining with dyes such as

35 tetrazolium dye and nitro blue tetrazolium (NBT), however, kinetic measurements have not been

36 performed. In the current study, we provide evidence of $O_2^{\bullet-}$ generation and its kinetics in the

37 leaves of spinach (*Spinacia oleracea*) subjected to wounding.

Methods:

39 Real-time monitoring of $O_2^{\bullet-}$ generation was performed using catalytic amperometry. Changes

40 in oxidation current for $O_2^{\bullet-}$ was monitored using polymeric iron-porphyrin-based modified

41 carbon electrodes (φ=1 mm) as working electrode with Ag/AgCl as the reference electrode.

Result:

42

43 The results obtained show a continuous generation of $O_2^{\bullet-}$ for minutes after wounding, followed

44 by a decline. The exogenous addition of superoxide dismutase, which is known to dismutate $O_2^{\bullet-}$

45 to H_2O_2, significantly suppressed the oxidation current.

46

Conclusion:

47

48   Catalytic amperometric measurements were performed using polymeric iron-porphyrin based

49   modified carbon electrode. It is claimed to be a useful tool and a direct method for real-time

50   monitoring and precise detection of $O_2^{\bullet-}$ in biological samples. It is claimed to bear a potential

51   for its wide application in plant research for specific and sensitive detection of $O_2^{\bullet-}$.

52

53

54

55

56

57

58

59

60

61

62

63

64

65

66

67

68

69

70   **INTRODUCTION**

71   The formation of reactive oxygen species (ROS) in plants is an unavoidable consequence

72   of photosynthesis [1-4]. The introduction of molecular oxygen into the environment by

73   photosynthetic organisms during the evolution of aerobic life is associated with the formation of

74   ROS [5]. Plants growing in a fluctuating environment are exposed to various biotic stresses such

75   as bacteria, viruses, fungi, parasites, insects, weeds, etc. and abiotic stresses such as fluctuations

76   in temperature, salinity, water, radiation, toxic chemicals and mechanical stress which are closely

77   linked to higher ROS production. The chloroplasts, mitochondria, and peroxisomes are among

78   the chief organelles involved [6-11]. As a response, ROS, including the superoxide anion radical

79   ($O_2^{\bullet-}$), hydroperoxyl radical ($HO_2^{\bullet-}$), hydrogen peroxide (H_2O_2), hydroxyl radical ($HO^{\bullet}$), singlet

80   oxygen ($^1O_2$), peroxyl radical ($ROO^{\bullet}$), hydroperoxide (ROOH) and alkoxyl radical ($RO^{\bullet}$), are

81   produced [12-18].

82   The production of ROS by an oxidative burst is an imperative element of the wound

83   response in algae, plants, and animals [19]. As a response to wounding, plants release

84   oligosaccharide cell wall fragments, which play an important role in the signaling cascade that

85   initiates an intense, localized production of ROS [20-22]. Wounding stimulates the production of

86    $O_2^{\bullet-}$, H_2O_2 and nitric oxide (NO), which can directly attack encroaching pathogens at the site of

87   the wound [23-25]. In *Arabidopsis thaliana* leaves measured under ambient light conditions, $O_2^{\bullet-}$

88   and H_2O_2 mainly originate from photosynthetic electron transport, predominantly at the site of

89   wounding [26]. The role of NADPH oxidase in ROS production, however, was not completely

90   ruled out. Therefore, the generation of $O_2^{\bullet-}$ and H_2O_2 can be attributed to the collective effect of

91   wounding and light stress. $O_2^{\bullet-}$ generation in the root cells of plants in response to wounding has

92   been studied by electron paramagnetic resonance (EPR) spin-trap spectroscopy and epinephrine-

93   adrenochrome acceptor methods [27]. Tiron (4, 5-dihydroxy-1, 3-benzene-disulfonic acid

94   disodium salt) was used, and the tiron semiquinone EPR spectra showed $O_2^{\bullet-}$ generation. The

95   level of $O_2^{\bullet-}$ production in the roots was measured with epinephrine which, in the presence of

96   $O_2^{\bullet-}$, is converted to adrenochrome and can be monitored at 480 nm by a spectrophotometer [28,

97   29]. In addition to spectroscopy, staining with dye, such as tetrazolium dye and nitro blue

98   tetrazolium (NBT), has been used to detect the production of $O_2^{\bullet-}$ *in situ*, with visualization of

99   $O_2^{\bullet-}$ generation as a purple formazan deposit within leaflet tissues [30].

100   Although various methods, such as EPR spin-trapping spectroscopy [31],

101   chemiluminescence [32], the reduction of NBT [37, 38] and the reduction of the redox protein

102   cytochrome c have been used to detect and monitor $O_2^{\bullet-}$, each of these methods has inadequate

103   specificity and sensitivity. EPR spin-trapping spectroscopy is one of the most sensitive and

104   specific method for ROS detection; however, kinetic measurements are not possible at the

105   current stage of development. Chemiluminescence, also known as ultra-weak photon emission,

106   has been widely used recently as a non-invasive method to understand the involvement of ROS

107   in oxidative radical reactions [36-38]; however, limitations with respect to the specificity for

108   particular ROS involvement exists [39].

109   Integration of metalloporphyrins into electropolymerized polymer electrodes have been

110   developed rigorously over the last years because these materials are effective electrocatalysts for

111   chemical as well as photochemical applications [40]. Numerous authors have recently tested the

112   potential use of electropolymerized metalloporphyrins as new electrode materials for chemical

113   and biological sensors [41-43]. In our current study, we provide an experimental approach for the

114   detection of $O_2^{\bullet-}$ by polymeric iron-porphyrin-based modified carbon electrode based on the

115   reaction mechanism presented in Fig. 1A (Yuasa & Oyaizu, 2005). Detection of $O_2^{\bullet-}$ by highly

116   sensitive and selective polymeric iron-porphyrin-based modified carbon electrodes was tested in

117 *in vivo* leaf sample subjected to wounding. The current study introduces the use of catalytic

118 amperometric biosensors for the real-time detection of $O_2^{\bullet-}$.

119

120 **MATERIAL AND METHODS**

121

122 *Spinach leaves*

123   Young spinach (*Spinacia oleracea)* leaves were washed twice with deionized water and

124 were dark adapted for 2 hours. For each measurement, a fresh spinach leaf of the approximately

125 same age was chosen. All experiments were performed at room temperature under dark

126 conditions to avoid interference from light sources.

127

128 *Material and chemical reagents*

129   The 5-(ethoxycarbonyl)-5-methyl-1-pyrroline N-oxide (EMPO) spin trap and capillary

130 tubes used for EPR measurements were obtained from Alexis Biochemicals (Lausen,

131 Switzerland) and Blaubrand intraMARK (Brand, Germany), respectively. The carbon electrodes

132 (φ=1 mm) were purchased from BAS Inc., ALS Co., Ltd. (Tokyo, Japan). Superoxide dismutase

133 (SOD), xanthine oxidase and xanthine (X/XO) were purchased from Wako Pure Chemicals

134 Industries, Ltd. (Osaka, Japan), Sigma-Aldrich chemie Gmbh (Munich, Germany) or Sigma-

135 Aldrich Japan K.K. (Tokyo, Japan).

136

137

138 *Equipment and methods*

139   Simultaneous measurements of the oxidation current of $O_2^{\bullet-}$ were performed using a

140   potentiostat (HA1010mM4S; Hokuto Denko Co., Ltd., Japan). The polymeric iron-porphyrin-

141   based modified carbon electrodes were positioned 1 mm from the site of injury using a motor-

142   driven XYZ-stage (K101-20MS-M, Suruga Seiki Co., Ltd., Japan) (Fig. 1B). The detection of

143    $O_2^{\bullet-}$ in the X/XO system was performed by EPR spin-trapping spectroscopy using 25 mM

144   EMPO in phosphate buffer.

145

146   ***Experimental conditions for real-time monitoring of the oxidation current of $O_2^{\bullet-}$***

147   The electrochemical detection of $O_2^{\bullet-}$ was measured using the X/XO system based on the

148   method described in our recent study [44] (Fig. 2). The subsequent oxidation current for $O_2^{\bullet-}$ was

149   monitored using polymeric iron-porphyrin-based modified carbon electrodes (φ=1 mm) with

150   Ag/AgCl as the reference electrode.

151   Spinach leaves were fixed on a petri-dish with a diameter of 60 mm using double-sided

152   adhesive tape. 10 mM Phosphate buffer saline (pH 7.2) (PBS) was gradually added to maintain a

153   sufficient volume to submerge the whole spinach leaf in PBS. During the measurement, injury

154   was performed using glass capillary with an inner diameter of about 1.2mm and wall thickness of

155   200μm as presented in Fig. 1B and DataS1. For data presented in the manuscript, the

156   injury/wounding in spinach leaves were done either 1 time or multiple times (between 8-10

157   times) while to visualize the state of leaves, injury/wounding was made 1 time, 5 times and 20

158   times (DataS1). Mechanical injury and mechanical wounding were performed close to the site of

159   the electrode. The oxidation current was measured at +0.5 V vs. Ag/AgCl at room temperature.

160

161 ***Superoxide anion radical detection using polymeric iron-porphyrin-based modified carbon***

162 ***electrodes***

163 The detection of $O_2^{\bullet-}$ was based on catalytic amperometry using a counter electrode and

164 working electrode. The counter electrode was a platinum wire ($\phi 0.25 \times 40$ mm), and the working

165 electrode ($\varphi 1$ mm) was a polymeric iron-porphyrin-based modified carbon electrode. Ag/AgCl

166 was used as a reference electrode. The polymeric iron-porphyrin-based modified carbon

167 electrode acted as an $O_2^{\bullet-}$ detection sensor. The polymeric iron-porphyrin-based modified carbon

168 electrode was prepared by the electropolymerization of 1-methylimidazole-coordinated

169 mesotetra (3-thienyl) porphyrin ([Fe(im)$_2$(ttp)]Br) (Yuasa & Oyaizu, 2005; Yuasa et al., 2005).

170 Electropolymerization was performed in a two-chamber three-electrode electrochemical cell by

171 potential cycling from 0 to +2.0 V vs. Ag/Ag$^+$ with a potential sweep rate of 50 mV s^{-1}. After

172 rinsing with dichloromethane, the polymeric iron-porphyrin-based modified carbon electrode

173 was obtained (Yuasa & Oyaizu, 2005; Yuasa et al., 2005). For the basic characterization of the

174 polymeric iron-porphyrin-based modified carbon electrode, a differential pulse voltammogram of

175 the electropolymerized [Fe(im)$_2$(ttp)]Br complex was recorded in an aqueous electrolyte solution

176 containing 10 mM PBS (pH 7.2) using a high-performance potentiostat HZ-7000 (Hokuto Denko

177 Co., Ltd., Japan) (supplementary data S2).

178

179 **RESULTS**

180 ***Characterization and sensitivity evaluation of an iron-porphyrin-based modified carbon***

181 ***electrode***

182 The characterization of the polymeric iron-porphyrin-based modified carbon electrode

183 was performed using a differential pulse voltammogram (DPV) (supplementary data S2). The

184 polymerized complex was electroactive, with a mean redox potential at -0.25 V for the Fe^{2+}/Fe^{3+}

185 couple.

186

187 ***Generation of $O_2^{\bullet-}$ in the chemical system and sensitivity evaluation of the polymeric iron-***

188 ***porphyrin-based modified carbon electrode***

189 The xanthine/xanthine oxidase system is used for the formation of $O_2^{\bullet-}$ by the reduction

190 of molecular oxygen [45-47]. To confirm the formation of $O_2^{\bullet-}$ in the chemical system used in

191 the later experimental procedures, we measured the EMPO-OOH adduct EPR signal

192 (supplementary data S3: A). The intensity of the EMPO-OOH adduct EPR signal in the control

193 (xanthine) and chemical system (X/XO) was also measured (supplementary data S3: B). In the

194 absence of xanthine oxidase, no EMPO-OOH adduct EPR signal was observed, whereas in the

195 presence of XO, an EMPO-OOH adduct EPR signal was observed (supplementary data S3).

196 To determine the sensitivity of the polymeric iron-porphyrin-based modified carbon

197 electrode, the response of the exogenous addition of a standard known concentration of $O_2^{\bullet-}$

198 generated *in situ* was measured using X/XO system. A linear increase in oxidation current was

199 observed with an increase in $O_2^{\bullet-}$ concentration. The calibration curve (Δi vs $O_2^{\bullet-}$) was found to

200 be linear in the concentration range of 0.4 to 1.3µM (Fig. 2). This indicates that the sensitivity of

201 the electrochemical sensor is in the range of µM concentration, reflecting changes in the

202 oxidation current in the order of tens of nA (Fig. 2).

203

204 ***Real-time monitoring of $O_2^{\bullet-}$ generation during wounding of spinach leaves***

205 To validate that there is no interference in the measurement caused by the suspension of

206 spinach leaf in PBS, the oxidation current was measured in a non-wounded spinach leaf

207   suspended in PBS (Fig. 3). No fluctuation in the oxidation current of $O_2^{\bullet-}$ was observed in the

208   non-wounded spinach leaf suspended in PBS, (Fig. 3), whereas a negligible fluctuation was

209   observed with the exogenous addition of SOD (data not shown). These results indicate that these

210   chemical species (PBS and SOD) do not interfere with the measurements. The kinetics of the

211   production of $O_2^{\bullet-}$ were also measured in the chemical system containing no spinach leaves and

212   in the presence of SOD (400 U ml^{-1}) indicating no significant fluctuation in oxidation current

213   (supplementary data S4).

214   Real-time monitoring of the oxidation current for $O_2^{\bullet-}$ was performed in spinach leaves

215   where mechanical injury was stimulated 1 time using glass tube (Fig. 4A) and mechanical

216   wounding was done multiple times (Fig. 4B). The wounding in spinach leaves was done 1 time

217   (4A) and multiple times (between 8-10 times) using a glass capillary with an inner diameter of

218   about 1.2mm and wall thickness of 200μm). The results indicate that the $O_2^{\bullet-}$ production

219   increased considerably with the dose of mechanical injury (Fig. 4). Furthermore, to visualize the

220   extent of damage to leaf during mechanical injury induced by glass capillary, photograph of

221   leaves showing the physiological state have been presented along with kinetics on real-time

222   monitoring of the oxidation current of $O_2^{\bullet-}$ under experimental condition mentioned in dataset

223   presented (Data S1). To determine the concentration of $O_2^{\bullet-}$ generated in mechanically injured

224   spinach leaves, the calibration curve was established for various concentrations obtained using

225   standard X/XO system (Fig. 2). A maximum oxidation current ($\triangle$i) of 1.5 nA (at time span, 60

226   sec) and 7.5 nA (at time span, 300 sec) was observed in mechanically injury made at a minimal

227   dose (Fig. 4A) and at multiple sites (Fig. 4B). Based on the data obtained and the maximum

228   oxidation current recorded, the $O_2^{\bullet-}$ was calculated and expected production was found to be

229   about 40 nM (4A) and 200 nM (4B) (Table 1).

230   In addition, $O_2^{\bullet-}$ generation was also measured in spinach leaves under the effect of

231   wounding at room temperature in presence of exogenous addition of SOD (Fig. 5). In the

232   absence of wounding, as observed during the first minute of real-time monitoring, no

233   considerable change in the oxidation currents of $O_2^{\bullet-}$ was observed. However, wounding

234   instantaneously resulted in a fast increase in the oxidation current for $O_2^{\bullet-}$ of approximately 10

235   nA, followed by a gradual decrease, which continued for more than 10 min. To confirm the

236   production of $O_2^{\bullet-}$, the effect of SOD, which leads to the dismutation of $O_2^{\bullet-}$ to H_2O_2, on the

237   oxidation current in a wounded spinach leaf was analyzed. The addition of 400 U ml^{-1} SOD

238   suppressed the oxidation current for $O_2^{\bullet-}$ from 3.5 nA to 2 nA (Fig. 5). However, complete

239   suppression of the oxidation current was not observed. The oxidation current, which persisted at

240   approximately 1 nA for a few minutes, can be attributed to rapid $O_2^{\bullet-}$ diffusion to the electrode

241   before its conversion to H_2O_2 or to the limited SOD activity at a fixed concentration. The effect

242   of SOD (400 U ml^{-1}) added exogenously was also measured at the point of maximum oxidation

243   current where a comparatively higher suppression was recorded (Fig. 6).

244

245   **DISCUSSION**

246   In addition to plants, ROS detections have been performed in model system including

247   animals. During recent past, Zuo and coworkers presented results on intracellular ROS formation

248   in single isolated frog myofibers during low P_{O2} conditions using dihydrofluorescein (Hfluor), a

249   fluorescein analog of DCFH [48,49]. Cyt c assay was also used to measure $O_2^{\bullet-}$ in contracting

250   skeletal muscle in pulmonary TNF-α overexpression mice [50, 51]. Several mechanisms for the

251   generation of ROS involving $O_2^{\bullet-}$ have been suggested. It has been proposed previously that an

252   NADPH oxidase-like enzyme in the plant plasma membrane is involved in the production of $O_2^{\bullet-}$,

253 which is then converted to the more stable H_2O_2 during the oxidative burst in response to

254 pathogen attack of plant cells [52, 53]. In skeletal muscle, the major source of ROS especially

255 extracellular $O_2^{\bullet-}$ formation is via the arachidonic acid metabolism through lipoxygenase (LOX)

256 activity [51]. However, in contrast to the view that wound-induced ROS are primarily produced

257 extracellularly by NADPH oxidase enzymes [54, 55], it has been recently indicated that wound-

258 induced $O_2^{\bullet-}$ and H_2O_2 originate from photosynthetic electron transport measured at wounded

259 sites under ambient light conditions [26]. The $O_2^{\bullet-}$ is produced during the electron transport

260 process by the reduction of molecular oxygen in the chloroplasts and mitochondria. The authors

261 proposed that $O_2^{\bullet-}$ and H_2O_2 production is linked to wounding, which is enhanced significantly

262 under light conditions.

263   A recent report on *Pisum sativum* seedlings proposes a mechanism responsible for

264 oxidative burst during wounding. During mechanical wounding, polyunsaturated fatty acids

265 (PUFA), polyamines, LOX and peroxidases (Prx) are released in the extracellular matrix. Under

266 these circumstances, LOX is involved in the oxidation of PUFA or polyamines, which induces

267 diamine oxidases (DAO) to produce H_2O_2, further leading to $O_2^{\bullet-}$ production catalyzed by Prx

268 [56]. A diverse range of organisms use Prx to produce $O_2^{\bullet-}$, e.g., *Triticum sativum* roots [57],

269 *Castanea sativa* and *Trichilia* seeds [58, 59], liverworts [60], and lichens [61]. Another group of

270 redox enzyme involved in the wound-induced oxidative burst is DAO [62-65], and cooperation

271 between DAO and Prx is considered important in the wound response. In addition to DAO and

272 Prx, LOX not only generates lipid hydroperoxides (LOOH) but can also generate $O_2^{\bullet-}$ via the

273 oxidation of pyridine nucleotides and therefore considerably contributes to oxidative stress in

274 cells [66]. Lipid oxidation by LOX is an important part of the wound-response because oxylipins,

275 the break-down products of lipid peroxides, can act as effective signaling molecules to rapidly

276   induce transcriptional changes during wounding [67, 68]. Plasma membrane-bound Prx can

277   utilize PUFA such as linoleic acid released at the wound site for the synthesis of $O_2^{\bullet-}$. Even if

278   LOX is not known to be directly involved in $O_2^{\bullet-}$ production, it was suggested that extracellular

279   LOX may play an important role by competing with Prx for fatty acids and producing reactive

280   electrophiles that coordinate signaling responses [53].

281   The electrochemical method with the employment of different modified electrodes have

282   been successfully standardized and applied for detection of varied ROS including $O_2^{\bullet-}$ during

283   the recent past [69-71]. The polymeric iron-porphyrin-based modified carbon electrode is a

284   useful tool and provides a direct method for real-time monitoring and precise detection of $O_2^{\bullet-}$ in

285   biological samples *in-situ* [71]. The kinetic measurement showing the production of $O_2^{\bullet-}$ for a

286   long   range   of   time   (minutes)   presented   in   our   study

287   (https://ecs.confex.com/ecs/229/webprogram/Paper70675.html) have been demonstrated and thus

288   opens a new area of investigation which have always been difficult to explore using other

289   available methods such as EPR spin trapping spectroscopy, fluorescence microscopy and other

290   biochemical methods etc. Thus, the electrode has strong potential for wide application in plant

291   research for the specific and sensitive detection of $O_2^{\bullet-}$ and the kinetic behavior in real-time. In

292   addition to points mentioned above, using synthetic porphyrin has an additional advantage. To

293   date, $O_2^{\bullet-}$ sensors based on naturally derived enzyme (e.g. SOD, Cyt. c) have been developed

294   [72]. However, enzymes on the sensor are likely to be denatured. In contrast, the porphyrin based

295   sensor can be used without denaturation. At the same time, the current method is cost effective.

296   Certain limitations exist; the current polymeric iron-porphyrin-based modified carbon electrodes

297   are light-sensitive, which might hinder its photo-electrochemical applicability [73]. In the current

298   study, we present our polymeric iron-porphyrin based modified carbon electrode for application

299   in real-time monitoring and precise detection of $O_2^{\bullet -}$ in biological system. It is claimed to bear a

300   potential for its wide application in plant research for specific and sensitive detection of $O_2^{\bullet -}$.

301

302

303   **FIGURE LEGENDS**

304   **Figure 1: Reaction mechanism and experimental setup.** (A) Schematic illustration of the

305   reaction mechanism for the amperometric detection of $O_2^{\bullet -}$using the polymeric iron-porphyrin-

306   based modified carbon electrode depicting the reduction-oxidation cycle leading to generation of

307   the oxidation current. (B) Schematic illustration of the experimental setup for the

308   electrochemical measurements. The stimulation was performed using a glass capillary, and the

309   polymeric iron-porphyrin-based modified carbon electron was positioned at a distance of 1 mm

310   using a motor-driven XYZmicroscopic stage (I). The *in vivo* generation of $O_2^{\bullet -}$was measured

311   using a polymeric iron-porphyrin-based modified carbon electron (working electrode, WE),

312   platinum wire (counter electrode, CE) and Ag/AgCl (reference electrode, RE) (II).

313   **Figure 2: Calibration curve.** Changes in oxidation current measured using iron-porphyrin-

314   based modified carbon electrode by exogenous addition of a standard known concentration of

315    $O_2^{\bullet -}$ generated *in situ* using X/XO system in the concentration range of 0.4 to 1.3μM.

316   **Figure 3: Real-time monitoring of the oxidation current of $O_2^{\bullet -}$from spinach leaves.** The

317   kinetics of the production of $O_2^{\bullet -}$was measured using a polymeric iron-porphyrin-based modified

318   carbon electrode on non-wounded spinach leaves.

319   **Figure 4: Real-time monitoring of oxidation current for $O_2^{\bullet -}$during wounding.** The kinetics

320   of the production of $O_2^{\bullet -}$ were measured using a polymeric iron porphyrin based modified carbon

321   electrode during wounding in spinach leaves. The wounding in spinach leaves was done 1 time

322   (A) and multiple times (B) close to the site of electrode during the measurement and oxidation

323   current for $O_2^{\bullet-}$ was measured.

324   **Figure 5: Real-time monitoring of the oxidation current of $O_2^{\bullet-}$ during wounding.** The

325   kinetics of the production of $O_2^{\bullet-}$ were measured using a polymeric iron-porphyrin-based

326   modified carbon electrode during wounding in spinach leaves. The wounding of spinach leaves

327   was performed during the measurement, and the oxidation current for $O_2^{\bullet-}$ was measured for

328   approximately 30 min. The effect of SOD on the oxidation current was measured in the presence

329   of SOD (400 U ml^{-1}) added exogenously during the measurement.

330   **Figure 6: Real-time monitoring of oxidation current for $O_2^{\bullet-}$ during wounding.** The kinetics

331   of the production of $O_2^{\bullet-}$ was measured using a polymeric iron porphyrin based modified carbon

332   electrode during wounding in spinach leaves. The wounding in spinach leaves was done during

333   the measurement and oxidation current for $O_2^{\bullet-}$ was measured for a duration of about 30 min.

334   Effect of SOD was measured in the presence of SOD (400U ml^{-1}) added exogenously during the

335   measurement at the point of maximum oxidation current.

336   **Table 1: Calculation.** Superoxide anion radical ($O_2^{\bullet-}$) concentration calculated using standard

337   calibration curve ($R^2 = 0.9918$) (Fig. 2). The total change in oxidation current was found to be 1.5

338   nA (Δi) for minimal dose of injury (Fig. 4A) and 7.5 nA (Δi) for injury at multiple sites (Fig. 4B).

339   The total $O_2^{\bullet-}$ concentration was found to be equivalent to 40 nM (Fig. 4A) and 200 nM (Fig.

340   4B) at 60 sec and 300 sec, respectively.

341

342   **SUPPLEMENTARY DATA**

343   ***Supplementary data S1:*** Photographs of glass capillary (4 nos.) each with an inner diameter of

344   about 1.2mm and wall thickness of 200μm used for inducing mechanical injury in spinach leaves.

345   **II.** (A) Photograph of Spinach leaves in the experimental setup. For each measurement, young

346   spinach leaves of size approximately 8-10mm were chosen. (B) Photographs of petriplate with

347   Spinach leaves showing the arrangement of electrodes. **III.** Photographs of Spinach leaves

348   showing its state after mechanical injury with glass capillary. Injury was made 1 time (A), 5

349   times (B) and 20 times (C). **IV.** The kinetics of the production of $O_2^{\bullet-}$ was measured using a

350   polymeric iron porphyrin based modified carbon electrode during wounding in spinach leaves

351   (arrow indicates mechanical wounding). The wounding in spinach leaves was done 20 times

352   close to the site of electrode during the measurement and oxidation current for $O_2^{\bullet-}$ was

353   measured.

354

355   ***Supplementary data S2:*** DPV for the electropolymerized [Fe(im)2(ttp)]Br complex recorded in

356   an aqueous electrolyte solution containing phosphate buffer (pH 7.2).

357

358   ***Supplementary data S3:*** EMPO-OOH adduct EPR spectra were measured in the presence of 25

359   mM EMPO, 40 mM phosphate buffer (pH 7.2) in the absence and presence of xanthine (1 mM)

360   and xanthine oxidase (0.2 U ml^{-1}). Panel (A) shows the spectra measured in the phosphate buffer

361   only (trace a) and X/XO system (trace b); (B) mean value ±SD, n=3, of the EMPO-OOH adduct

362   EPR spectra. The intensity of the EPR signal depicted in (B) was evaluated by measuring the

363   relative height of the central peak of the first derivative of the EPR absorption spectrum.

364

365 ***Supplementary data S4:*** Kinetics of the production of $O_2^{\bullet-}$ was measured using polymeric iron

366 porphyrin based modified carbon electrode in the chemical system (phosphate buffer) in the

367 presence of SOD (400U ml-1).

368

369 **REFERENCES**

370 1. Ledford HK, Chin BL, and Niyogi KK. Acclimation to singlet oxygen stress in

371 Chlamydomonas reinhardtii. Eukaryotic Cell. 2007; 6: 919–930.

372 2. Alessandro A, Osto LD, Aprile A, Carillo P, Roncaglia E, Cattivelli L, Bassi R. Reactive

373 oxygen species and transcript analysis upon excess light treatment in wild-

374 type *Arabidopsis thaliana* vs a photosensitive mutant lacking zeaxanthin and lutein. BMC

375 Plant Biology. 2011; 11: 62.

376 3. Foyer CH, and Shigeoka S. Understanding Oxidative Stress and Antioxidant Functions to

377 Enhance Photosynthesis. Plant Physiology. 2011; 155: 93–100.

378 4. Laloi C, and Havaux M. Key players of singlet oxygen-induced cell death in plants.

379 Frontiers in Plant Science. 2015; 6: 39.

380 5. Tripathy BC, Oelmüller R. Reactive oxygen species generation and signaling in plants.

381 Plant Signaling and Behavior. 2012; 7(12): 1621–1633.

382 6. Elstner EF. Mechanisms of oxygen activation in different compartments of plant cells,

383 in Active Oxygen/Oxidative Stress and Plant Metabolism, E. J. Pell and K. L. Steffen,

384 Eds., pp. 13–25, American Society of Plant Physiologists, Rockville, Md, USA. 1991.

385 7. Foyer CH, and Harbinson J. "Oxygen metabolism and the regulation of photosynthetic

386 electron transport," in Causes of Photooxidative Stresses and Amelioration of Defense

387   Systems in Plants, C. H. Foyer and P. Mullineaux, Eds., pp. 1–42, CRC Press, Boca

388   Raton, Fla, USA. 1994.

389   8. Asada K. Radical production and scavenging in the chloroplasts," in Photosynthesis and

390   the Environment, N. R. Baker, Ed., pp. 123–150, Kluwer, Dordrecht, The Netherlands.

391   1996.

392   9. Turrens JF. Mitochondrial formation of reactive oxygen species. Journal of Physiology.

393   2003; 552: 335–344.

394   10. Liu Y, Ren D, Pike S, Pallardy S, Gassmann W, and Zhang S. Chloroplast-generated

395   reactive oxygen species are involved in hypersensitive response-like cell death mediated

396   by a mitogen-activated protein kinase cascade. Plant Journal. 2007; 51: 941–954.

397   11. Murphy MP. How mitochondria produce reactive oxygen species. Biochemical Journal.

398   2009; 417: 1–13.

399   12. Miller G, Shulaev V, Mittler R. Reactive oxygen signaling and abiotic stress. Physiologia

400   Plantarum. 2008; 133(3): 481–489.

401   13. Gill SS, and Tuteja N. Reactive oxygen species and antioxidant machinery in abiotic

402   stress tolerance in crop plants. Plant Physiology and Biochemistry. 2010; 48: 909–930.

403   14. Foyer CH, Noctor G. Redox homeostasis and antioxidant signaling: a metabolic interface

404   between stress perception and physiological responses. Plant Cell. 2005; 17: 1866–1875.

405   15. Asada K. Production and scavenging of reactive oxygen species in chloroplasts and their

406   functions. Plant Physiology. 2006; 141: 391–396.

407   16. Miller G, Schlauch K, Tam R, Cortes D, Torres MA, Shulaev V, Dangl JL, Mittler R.

408   The plant NADPH oxidase RBOHD mediates rapid systemic signaling in response to

409   diverse stimuli. Science Signaling. 2009; 2(84): 45–49.

410   17. Bhattacharjee S. Sites of generation and physicochemical basis of formation of reactive

411   oxygen species in plant cell, in Reactive Oxygen Species and Antioxidants in Higher

412   Plants. S. Dutta Gupta, Ed., pp. 1–30, CRC Press, New York, NY, USA. 2010.

413   18. Choudhury S, Panda P, Sahoo L, and Panda SK. Reactive oxygen species signalling in

414   plants under abiotic stress. Plant Signaling & Behaviour. 2013; 8: e23681.

415   19. McDowell RE, Amsler MO, Li Q, Lancaster Jr JR, Amsler CD. The immediate wound-

416   induced oxidative burst of Saccharina latissimi depends on light via photosynthetic

417   electron transport. Journal of Phycology. 2015; 51: 431–441.

418   20. Legendre L, Rueter S, Heinstein PF, Low PS. Characterization of the oligogalacturonide-

419   induced oxidative cells. Plant Physiology. 1993; 102: 233–240.

420   21. John M, Rohrig G, Schmidt J, Walden R, Schell J. Cell signaling by oligosaccharides.

421   Trends in Plant Science. 1997; 2: 111–115.

422   22. Stennis M, Chandra S, Ryan C, Low P. Systemin potentiates the oxidative burst in

423   cultured tomato cells. Plant Physiology. 1998; 117: 1031–1036.

424   23. Murphy TM, Asard H, Cross AR. Possible sources of reactive oxygen during the

425   oxidative burst in plants. In: Asard, H., Berczi, A. (Eds.), Plasma Membrane Redox

426   Systems and their Role in Biological Stresses and Disease. Kluwer Academic Publishers,

427   Dordrecht, pp. 215–246. 1998.

428   24. Garces H, Durzan D, Pedroso MC. Mechanical stress elicits nitric oxide formation and

429   DNA fragmentation in *Arabidopsis thaliana*. Annals of Botany. 2001; 87: 567–574.

430   25. Jih PJ, Chen YC, Jeng ST. Involvement of hydrogen peroxide and nitric oxide in

431   expression of the ipomoelin gene from sweet potato. Plant Physiology. 2003; 132: 381–

432   389.

433 26. Morker KH, Roberts MR. Light as both an input and an output of wound-induced

434   reactive oxygen formation in Arabidopsis leaves. Plant Signaling and Behaviour. 2011;

435   6(8): 1-3.

436 27. Vylegzhaninat NN, Gordon LK, Minibayeva FV, Kolesnikov OP. Superoxide Production

437   as a Stress Response of Wounded Root Cells: ESR Spin-Trap and Acceptor Methods.

438   Applied Magnetic Resonance. 2001; 21: 63-70.

439 28. Misra HR, Fridovich I. The Univalent Reduction of Oxygen by Reduced Flavins and

440   Quinones. The Journal of Biological Chemistry. 1972; 247: 188-192.

441 29. Barber MJ, Kay CJ. Superoxide production during reduction of molecular oxygen by

442   assimilatory nitrate reductase. Archives of Biochemistry and Biophysics. 1996; 326: 227-

443   232.

444 30. Wohlgemuth H, Mittelstrass K, Kschieschan S, Bender J, Weigel HJ, Overmyer K,

445   Kangasjärvi J, Sandermann H, Langebartels C. Activation of an oxidative burst is a

446   general feature of sensitive plants exposed to the air pollutant ozone. Plant Cell

447   Environment. 2002; 25: 717–726.

448 31. Von GM, Schlosser E, Neubacher H. Evidence from electron-spin resonance for the

449   formation of free radicals during infection of Avena sativa by Drechslera spp. Physiology

450   and Molecular Plant Pathology. 1993; 42: 405–412.

451 32. Anderson AA, Rogers K, Tepper CS, Blee K, Cardon J. Timing of molecular events

452   following elicitor treatment of plant cells. Physiology and Molecular Plant Pathology

453   1991; 38: 1–13.

454   33. Doke N. Involvement of superoxide anion generation in the hypersensitive response of

455   potato tuber tissues to infection with an incompatible race of Phytophthora infestans and

456   to the hyphal wall components. Physiological Plant Pathology. 1983; 23: 345–357.

457   34. Doke N. Generation of superoxide anion by potato tuber protoplasts during the

458   hypersensitive response to hyphal wall components of Phytophthora infestans and

459   specific inhibition of the reaction by suppressors of hypersensitivity. Physiological Plant

460   Pathology. 1983; 23: 359–367.

461   35. Doke N. NADPH-dependent $O_2^{\bullet-}$ generation in membrane fractions isolated from

462   wounded potato tubers inoculated with Phytophthora infestans. Physiological Plant

463   Pathology. 1985; 27: 311–322.

464   36. Prasad A and Pospíšil P. Ultraweak photon emission induced by visible light and

465   ultraviolet A radiation via photoactivated skin chromophores: in vivo charge coupled

466   device imaging. Journal of Biomedical Optics. 2012; 17(8): 85004.

467   37. Prasad A and Pospíšil P. Towards the two-dimensional imaging of spontaneous ultra-

468   weak photon emission from microbial, plant and animal cells. Scientific Reports. 2013; 3:

469   1211.

470   38. Pospíšil P, Prasad A and Rác M. Role of reactive oxygen species in ultra-weak photon

471   emission in biological systems. Journal of Photochemistry and Photobiology B: Biology

472   .2014; 139: 11-23.

473   39. Halliwell B, Gutteridge JMC. Free Radicals in Biology and Medicine, Ed 2. Clarendon

474   Press, Oxford, UK. 1989.

475 40. Bedioui F, Devynck J and Charreton CB. Immobilization of metalloporphyrins in
476   electropolymerized films: design and applications. Accounts of Chemical Research.
477   1995; 28 (1), 30-36

478 41. Deronzier A, and Moutet JC. Polypyrrole films containing metal complexes: syntheses
479   and applications. Coordination Chemistry Reviews. 1996; 147, 339-371.

480 42. Yim HS, Kibbey CE, Ma SC, Kliza DM, Liu D, Park SB, Terre CE and Meyerhoff ME.
481   Polymer membrane-based ion-, gas- and bio-selective potentiometric sensors. Biosensors
482   and Bioelectronics. 1993; 8,1-38.

483 43. Bedioui F, Trevin S, and Devynck J. Chemically modified microelectrodes designed for
484   the electrochemical determination of nitric oxide in biological systems. Electroanalysis.
485   1996; 8, 1085-1091.

486 44. Matsuoka R, Igarashi M, Kondo T, Aikawa T, and Yuasa M. Biomimetic
487   antithrombogenic electrochemical superoxide anion radical sensor. Journal of the
488   Electrochemical Society. 2014; 161:6.

489 45. Olson JS, Ballou DP, Palmer GS, Massey V. The Reaction of Xanthine Oxidase with
490   Molecular Oxygen. The Journal of Biological Chemistry. 1974; 249: 4350-4362.

491 46. Richter C. Redox intermediates between O_2 and H_2O. Membrane Biochemistry. A
492   Laboratory Manual on Transport and Bioenergetics. doi: 10.1007/978-3-642-67530-0_12.
493   1979.

494 47. Porras AG, Olson JS, Palmer G. The reaction of reduced xanthine oxidase with oxygen.
495   Kinetics of peroxide and superoxide formation. The Journal of Biological Chemistry.
496   1981; 256: 9096-9103.

497   48. Zuo L, Nogueira L and Hogan MC. Reactive oxygen species formation during tetanic

498   contractions in single isolated Xenopus myofibers. Journal of Applied Physiology. 2011;

499   111: 898-904.

500   49. Zuo L, Shiah A, Roberts WJ, Chien MT, Wagner PD and Hogan MC. Low P_{O2}

501   Conditions Induce Reactive Oxygen Species Formation during Contractions in Single

502   Skeletal Muscle Fibers. American Journal of Physiology. Regulatory, integrative and

503   Comparative Physiology. 2013; 304 (11): R1009-16.

504   50. Zuo L, Hallman AH, Roberts WJ, Wagner PD, Hogan MC. Superoxide release from

505   contracting skeletal muscle in pulmonary TNF-α overexpression mice. American Journal

506   of Physiology. Regulatory, integrative and Comparative Physiology. 2014; 306(1): R75-

507   R81.

508   51. Zuo L, Christofi FL, Wright VP, Bao S, Clanton TL. Lipoxygenase-dependent

509   superoxide release in skeletal muscle. Journal of Applied Physiology. 2004; 97(2):661-

510   668.

511   52. Murphy TM, Auh CK. The Superoxide Synthases of Plasma Membrane Preparations

512   from Cultured Rose Cells. Plant Physiology. 1996; 110: 621-629.

513   53. Doke N, Miura J, Sanchez LM, Park HJ, Noritake T, Yoshioka H, Kawakita K. The

514   oxidative burst protects plants against pathogen attack: mechanism and role as an

515   emergency signal for plant bio-defence- a review. Gene. 1996; 179: 45-5.

516   54. Watanabe T, Sakai S. Effects of active oxygen species and methyl jasmonate on

517   expression of the gene for a wound-inducible 1-aminocyclopropane-1-carboxylate

518   synthase in winter squash (C. maxima). Planta. 1998; 206: 570-576.

519   55. Flor-Henry M, McCabe TC, Bruxelles GL de, Roberts MR. Use of a highly sensitive

520   two-dimensional luminescence imaging system to monitor endogenous bioluminescence

521   in plant leaves. BMC Plant Biology. 2004; 4: 19.

522   56. Roach T, Colville L, Beckett RP, Minibayeva FV, Havaux M, Kranner I. A proposed

523   interplay between peroxidase, amine oxidase and lipoxygenase in the wounding-induced

524   oxidative burst in Pisum sativum seedlings. Phytochemistry. 2015; 112: 130–138.

525   57. Minibayeva F, Kolesnikov O, Chasov A, Beckett RP, Luthje S, Vylegzhanina N, Buck F

526   and Bottger M. Wound-induced apoplastic peroxidases activities: their roles in the

527   production and detoxification of reactive oxygen species. Plant Cell Environment. 2009;

528   32: 497–508.

529   58. Roach T, Beckett RP, Minibayeva FV, Colville L, Whitaker C, Chen H, Bailly C,

530   Kranner I. Extracellular superoxide production, viability and redox poise in response to

531   desiccation in recalcitrant Castanea sativa seeds. Plant Cell Environment. 2009; 33: 59–

532   75.

533   59. Whitaker C, Beckett RP, Minibayeva FV, Kranner I. Production of reactive oxygen

534   species in excised, desiccated and cryopreserved explants of Trichiliadregeana. South

535   African Journal of Botany. 2010; 76: 112–118.

536   60. Li JLY, Sulaiman M, Beckett RP, Minibayeva FV. Cell wall peroxidases in the liverwort

537   Dumortiera hirsuta are responsible for extracellular superoxide production, and can

538   display tyrosinase activity. Physiologia Plantarum. 2010; 138: 474–484.

539   61. Liers C, Ullrich C, Hofrichter M, Minibayeva FV, Beckett RP. Oxidoreductases from

540   lichenized ascomycetes: purification and characterization of a heme-peroxidase from

541   Leptogium saturninum that oxidizes high-redox potential substrates. Fungal Genetics and

542   Biology 2011; 48: 1139–1145.

543   62. Rea G, Metoui O, Infantino A, Federico R, Angelini R. Copper amine oxidase expression

544   in defense responses to wounding and Ascochyta rabiei invasion. Plant Physiology. 2002;

545   128: 865–875.

546   63. Cona A, Rea G, Botta M, Corelli F, Federico R, Angelini R. Flavin containing polyamine

547   oxidase is a hydrogen peroxide source in the oxidative response to the protein

548   phosphatase inhibitor cantharidin in Zea mays L. Journal of Experimental Botany. 2006;

549   57: 2277–2289.

550   64. Yoda H, Hiroi Y, Sano H. Polyamine oxidase is one of the key elements for oxidative

551   burst to induce programmed cell death in tobacco cultured cells. Plant Physiology. 2006;

552   142: 193–206.

553   65. Angelini R, Tisi A, Rea G, Chen MM, Botta M, Federico R, Cona A. Involvement of

554   polyamine oxidase in wound healing. Plant Physiology. 2008; 146: 162–177.

555   66. Roy P, Roy SK, Mitra A, Kulkarni AP. Superoxide generation by lipoxygenase in the

556   presence of NADH and NADPH. Biochimica et Biophysica Acta. 1994; 1214: 171–179.

557   67. Upchurch RG. Fatty acid unsaturation, mobilization, and regulation in the response of

558   plants to stress. Biotechnology Letters. 2008; 30: 967–977.

559   68. Higdon A, Diers AR, Oh, J, Landar Y, Darley-Usmar VM. Cell signalling by reactive

560   lipid species: new concepts and molecular mechanisms. Biochemical Journal. 2012; 442:

561   453–464.

562   69. Groenendaal Jonas F, Freitag D, Pielartzik H, and Reynolds JR. Poly(3,4

563   ethylenedioxythiophene) and Its Derivatives: Past, Present, and Future. Advanced

564   Materials. 2000; 12: 481.

565   70. Yuasa, M and Oyaizu, K. Electrochemical Detection and Sensing of Reactive Oxygen

566   Species. Current Organic Chemistry. 2005; 9: 1685.

567   71. Yuasa M, Oyaizu K, Yamaguchi A, Ishikawa M, Eguchi K, Kobayashi T, Toyoda Y, and

568   Tsutsui S. Electrochemical sensor for superoxide anion radical using polymeric iron

569   porphyrin complexes containing axial 1-methylimidazole ligand as cytochrome c mimics.

570   Polymers for Advanced Technologies. 2005; 16: 287-292.

571   72. Di J, Bi S, Zhang M. Third-generation superoxide anion sensor based on superoxide

572   dismutase directly immobilized by sol–gel thin film on gold electrode. Biosensors and

573   Bioelectronics. 2004; 19: 1479–1486.

574   73. Brett CMA and Brett AMCFO. Surface modified electrode-reasons and advantages"

575   in Surface Engineering: Surface modification of materials, R. Kossowsky and S.C.

576   Singhal, Ed., pp. 656–664, Westinghouse R &D center, Pittsburg, USA. 1984.

577   74. Prasad A, Kikuchi H, Inoue KY, Suzuki M, Sugiura Y, Sugai T, Tomonori A, Tada M,

578   Kobayashi M, Matsue T and Kasai S. Simultaneous Real-Time Monitoring of Oxygen

579   Consumption and Hydrogen Peroxide Production in Cells Using Our Newly Developed

580   Chip-Type Biosensor Device. Frontiers in Physiology. 2016; 7: 109.

Calculation

Superoxide anion radical ($O_2{}^{\bullet-}$) concentration calculated using standard calibration curve ($R^2 = 0.9918$) (Fig. 2). The total change in oxidation current was found to be 1.5 nA (Δi) for minimal dose of injury (Fig. 4A) and 7.5 nA (Δi) for injury at multiple sites (Fig. 4B). The total $O_2{}^{\bullet-}$ concentration was found to be equivalent to 40 nM (Fig. 4A) and 200 nM (Fig. 4B) at 60 sec and 300 sec, respectively.

	A	B
Δi (nA)	1.5	7.5
Δt (sec)	60	300
$O_2^{\bullet-}$ (nM)	**40**	**200**

Reaction mechanism and experimental setup.

(A) Schematic illustration of the reaction mechanism for the amperometric detection of $O_2^{\bullet-}$ using the polymeric iron-porphyrin-based modified carbon electrode depicting the reduction-oxidation cycle leading to generation of the oxidation current. (B) Schematic illustration of the experimental setup for the electrochemical measurements. The stimulation was performed using a glass capillary, and the polymeric iron-porphyrin-based modified carbon electron was positioned at a distance of 1 mm using a motor-driven XYZmicroscopic stage (I). The *in vivo* generation of $O_2^{\bullet-}$ was measured using a polymeric iron-porphyrin-based modified carbon electron (working electrode, WE), platinum wire (counter electrode, CE) and Ag/AgCl (reference electrode, RE) (II).

A
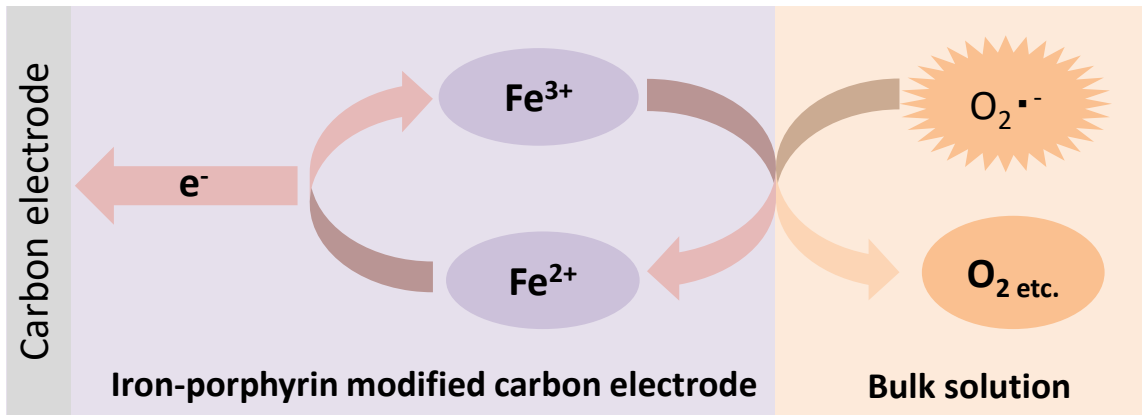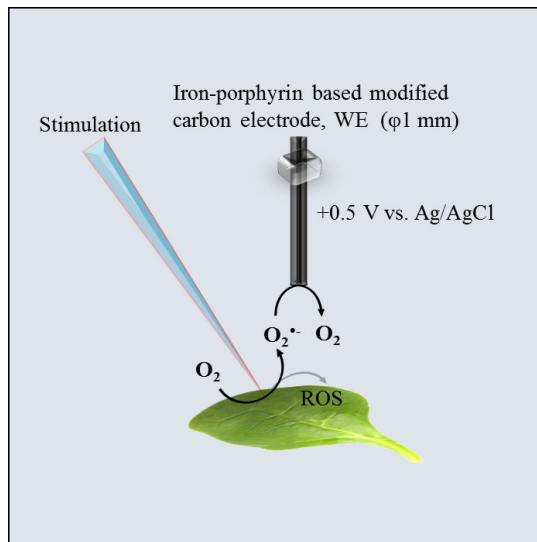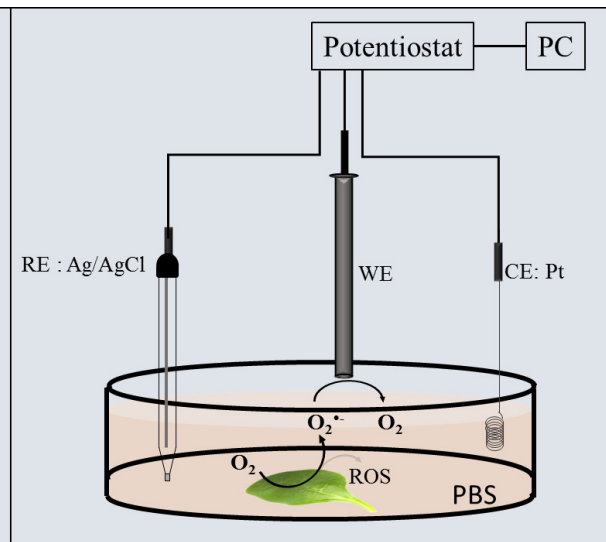
Carbon electrode

Iron-porphyrin modified carbon electrode

Fe^{3+}

e^-

Fe^{2+}

$O_2^{\bullet-}$

$O_{2\ etc.}$

Bulk solution

B

Stimulation

Iron-porphyrin based modified carbon electrode, WE (φ1 mm)

+0.5 V vs. Ag/AgCl

$O_2^{\bullet-}$ O_2

O_2

ROS

C

Potentiostat — PC

RE : Ag/AgCl

WE

CE: Pt

$O_2^{\bullet-}$ O_2

O_2

ROS

PBS

Calibration curve

Changes in oxidation current measured using iron-porphyrin-based modified carbon electrode by exogenous addition of a standard known concentration of $O_2^{\cdot-}$ generated *in situ* using X/XO system in the concentration range of 0.4 to 1.3µM.
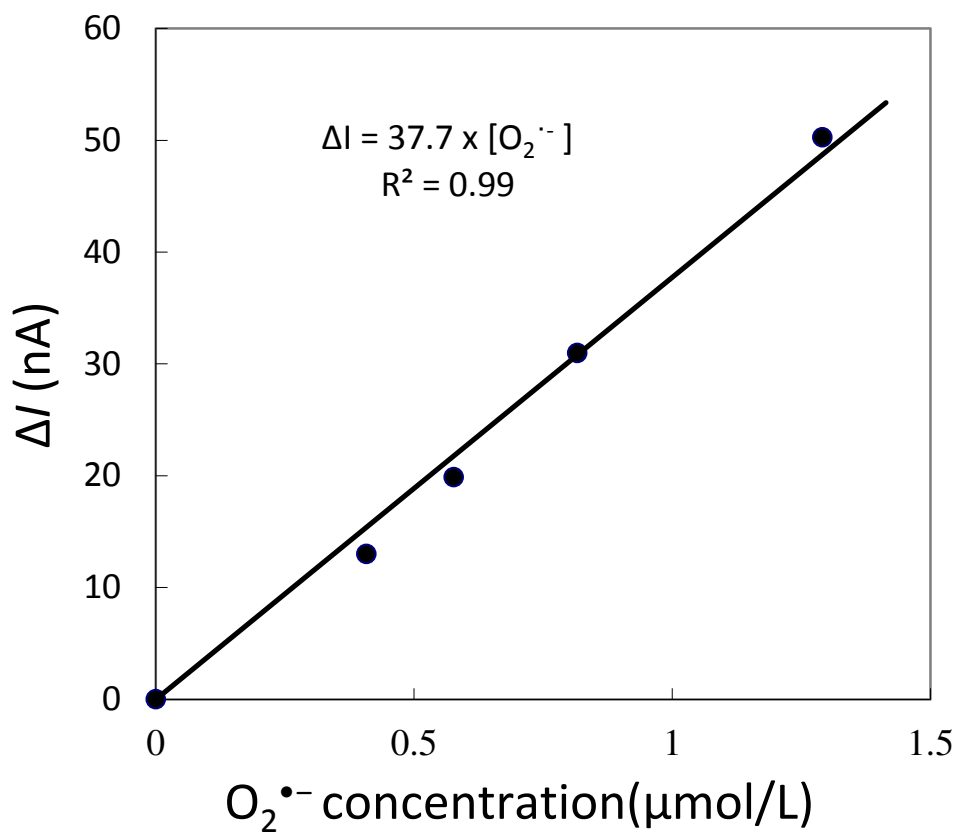
Real-time monitoring of the oxidation current of $O_2{}^{\bullet-}$ from spinach leaves.

The kinetics of the production of $O_2{}^{\bullet-}$ was measured using a polymeric iron-porphyrin-based modified carbon electrode on non-wounded spinach leaves.
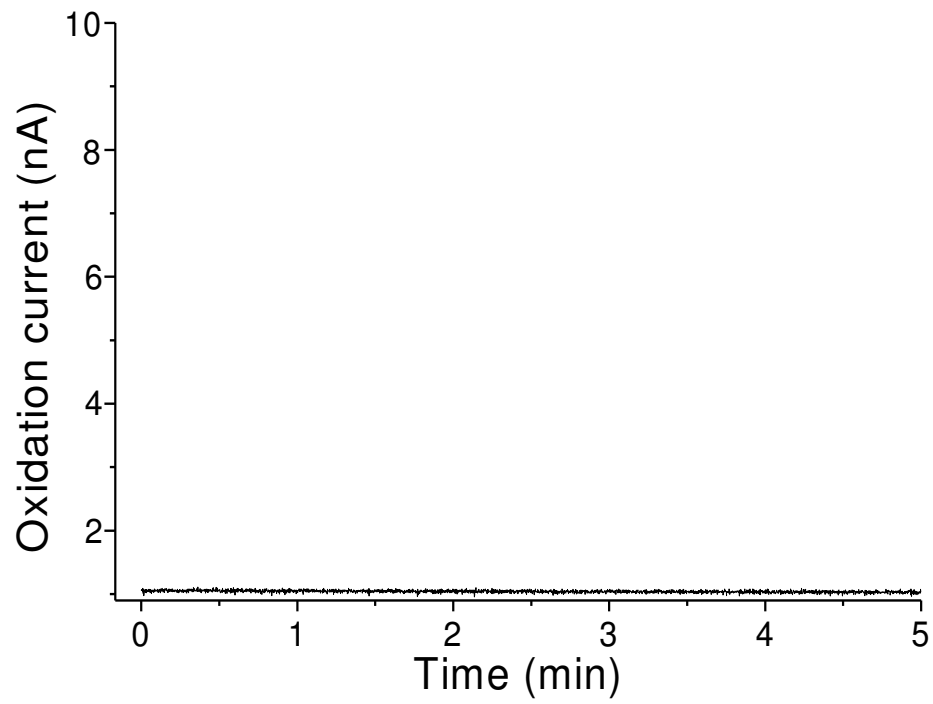
Real-time monitoring of oxidation current for $O_2^{\bullet-}$ during wounding

The kinetics of the production of $O_2^{\bullet-}$ were measured using a polymeric iron porphyrin based modified carbon electrode during wounding in spinach leaves. The wounding in spinach leaves was done 1 time (A) and multiple times (B) close to the site of electrode during the measurement and oxidation current for $O_2^{\bullet-}$ was measured.
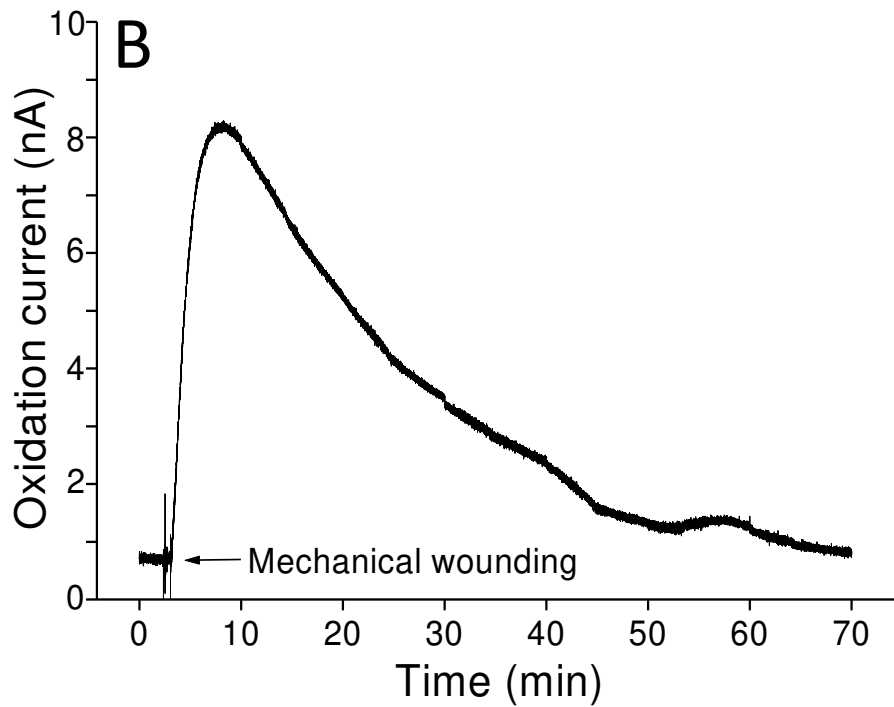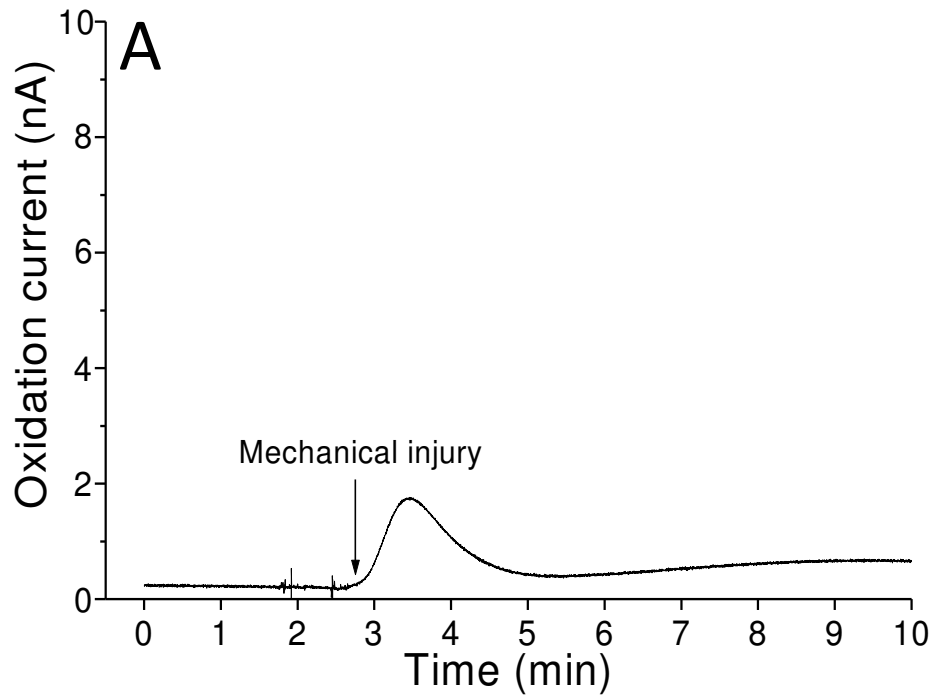
Real-time monitoring of the oxidation current of $O_2{}^{\bullet-}$during wounding

The kinetics of the production of $O_2{}^{\bullet-}$were measured using a polymeric iron-porphyrin-based modified carbon electrode during wounding in spinach leaves. The wounding of spinach leaves was performed during the measurement, and the oxidation current for $O_2{}^{\bullet-}$was measured for approximately 30 min. The effect of SOD on the oxidation current was measured in the presence of SOD (400 U ml^{-1}) added exogenously during the measurement.
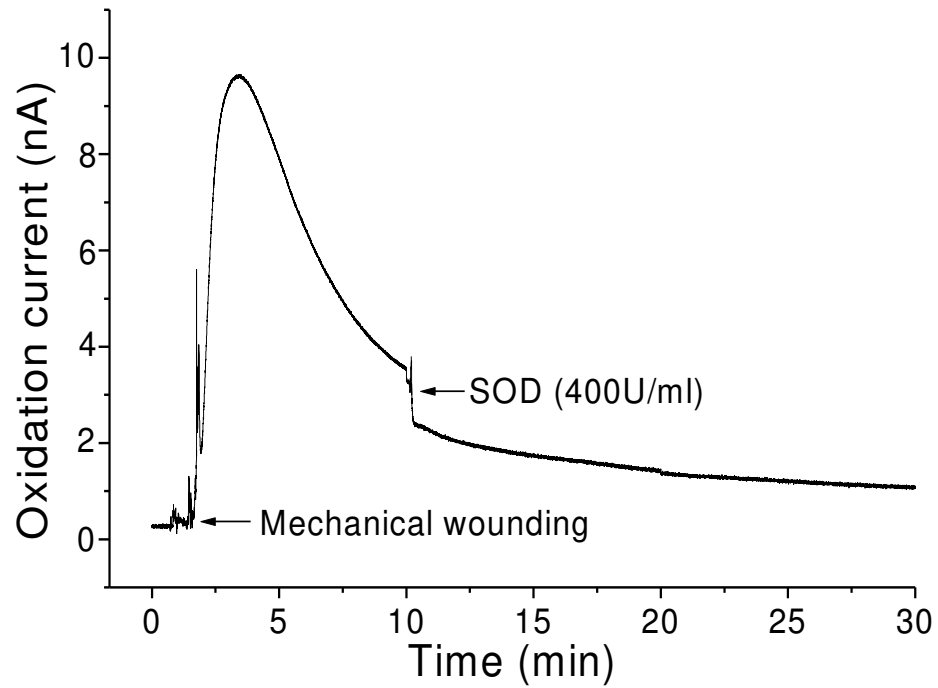
Real-time monitoring of oxidation current for $O_2^{\bullet-}$ during wounding.

The kinetics of the production of $O_2^{\bullet-}$ was measured using a polymeric iron porphyrin based modified carbon electrode during wounding in spinach leaves. The wounding in spinach leaves was done during the measurement and oxidation current for $O_2^{\bullet-}$ was measured for a duration of about 30 min. Effect of SOD was measured in the presence of SOD (400U ml^{-1}) added exogenously during the measurement at the point of maximum oxidation current.